ISBN: 978-3-95450-261-5 ISSN: 2673-7000 doi: 10.18429/JACoW-NAPAC2025-TUP050

IMPACT OF ELECTRON BEAM SIZE RIPPLE ON PROTON EMITTANCE GROWTH FOR EIC*

D. Xu†, Y.-K. Kan, Y. Luo, B. Podobedov
Brookhaven National Laboratory, Upton, NY, USA

Abstract

The Electron-Ion Collider (EIC) employs a flat hadron beam to achieve high luminosity, with the proton beam's vertical emittance being an order of magnitude smaller than its horizontal one. The smaller vertical emittance is sensitive to external noise. This study examines electron beam size ripple, which comes from power supply fluctuations. Through beam-beam interaction, the electron size ripple contributes to vertical emittance growth. Mitigation strategies are discussed to preserve the flat beam aspect ratio.

INTRODUCTION

The Electron-Ion Collider (EIC) is a next-generation facility to be constructed at Brookhaven National Laboratory (BNL) [1]. The EIC employs flat hadron beam to achieve high luminosity [2], in which the vertical emittance of the proton beam is ten times smaller than the horizontal one.

This configuration introduces sensitivities to external noise, particularly in the vertical plane. One such concern is the electron beam size ripple. Due to the nonlinear beam-beam interactions, fluctuations in the electron beam size can induce a time-varying beam-beam force on the protons. When this force resonates with the betatron or synchro-betatron motion of the proton beam, it can drive vertical emittance growth, compromising the flatness of the hadron beam.

This paper investigates the impact of electron beam size ripple on proton emittance evolution using weak-strong beam-beam simulations. The ripple modeling and simulation setup follow our previous study on electron orbit ripple [3], with the key distinction that the fluctuation is applied to the RMS beam size of the strong beam rather than its centroid position. Simulation results show that even small ripples can cause cumulative emittance growth, depending on their frequency and amplitude. Possible mitigation strategies are discussed to reduce the vertical emittance growth.

FULL RANGE SCAN OF CENTER FREQUENCY

Figure 1 presents the results of a frequency scan with an electron beam size ripple of 0.5%. The ripple amplitude is defined as the RMS variation of the electron beam size, normalized to the nominal beam sizes at the interaction point (IP). The proton working point is $\nu_x = 0.228$, $\nu_y = 0.210$, and $\nu_z = -0.01$. The ripple is modeled as narrow-band noise with a bandwidth of 1000 Hz, which is slightly larger than the beam-beam tune spread. The center frequency of this ripple is scanned from 0 up to half the revolution frequency.

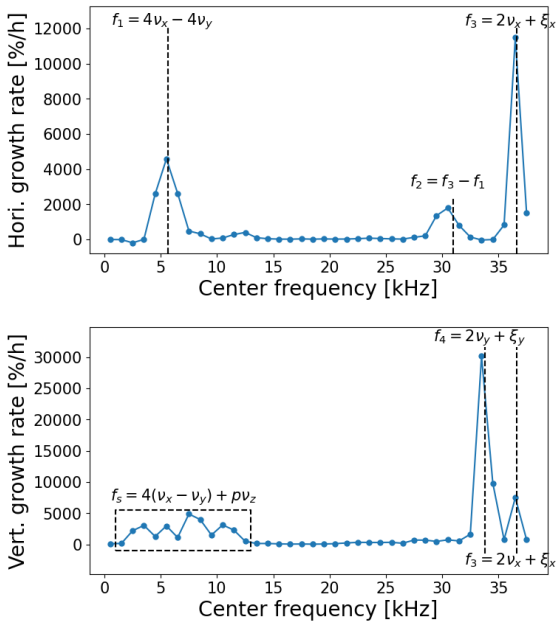

Figure 1: Proton horizontal (top) and vertical (bottom) emittance growth rates as a function of ripple frequency, with a fixed electron size ripple amplitude of $0.5\%\sigma_{x,y}$. The vertical lines and labeled numbers indicate resonance conditions (frequencies normalized by the revolution frequency). Simulations are tracked for 10^6 turns.

In the horizontal plane, the dominant peak appears at $f_3 = 2\nu_x$, corresponding to envelope oscillations of the proton beam. Due to the beam-beam tune spread $\xi_x \sim 0.1$, this peak spans from $2\nu_x$ to $2\nu_x + 2\xi_x$. This resonance occurs because the external ripple frequency aligns with the envelope oscillation frequency of the proton beam, which is twice the horizontal betatron frequency.

The second strongest peak occurs at $f_1 = 4\nu_x - 4\nu_y$, which is interpreted as a harmonic of the cross-plane coupling resonance $2\nu_x - 2\nu_y$. Since the beam-beam potential is an even function of transverse coordinates $V_{bb} = V(x^2, y^2)$, and the size ripple drives envelope oscillations at twice the betatron frequency, this resonance drives a large emittance growth when the external frequency coincides with it.

The third peak, located at $f_2 = f_3 - f_1$, may correspond to a sideband arising from the interference between the primary envelope mode and the nonlinear coupling mode.

Similarly, in the vertical plane, the highest peak appears at twice the vertical betatron frequency, $f_4 = 2\nu_y$, corresponding to vertical envelope oscillations. Since the verti-

* Work supported by Brookhaven Science Associates, LLC under Contract No. DE-SC0012704 with the U.S. Department of Energy.
† dxu@bnl.gov

ISBN: 978-3-95450-261-5 ISSN: 2673-7000 doi: 10.18429/JACoW-NAPAC2025-TUP050

cal emittance is much smaller than the horizontal one, the vertical emittance evolution is also sensitive to horizontal resonances due to nonlinear beam-beam coupling. As a result, a secondary peak emerges at the horizontal envelope frequency, $f_3 = 2\nu_x$.

A more complex pattern arises near the low-frequency region, where multiple peaks are observed. These can be attributed to synchro-betatron resonances of the form

$$f_5 = 4(\nu_x - \nu_y) + p\nu_z$$

where p is an integer. These resonances are intrinsic to the nonlinear beam-beam interaction and represent synchro-betatron sidebands of the betatron coupling. When the external ripple frequency matches one of these sidebands, vertical emittance growth can be resonantly excited.

UNDER 1200 Hz

Electron beam size ripple primarily originates from fluctuations in the quadrupole power supplies. While the most dangerous frequencies correspond to twice the proton betatron frequencies, the actual ripple amplitude at these high frequencies is significantly attenuated by several orders of magnitude, due to shielding effects from the copper vacuum chamber and other effects [4].

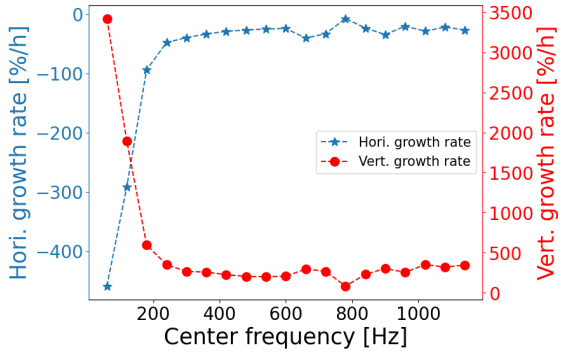

Figure 2: Emittance growth rates under a 5% electron beam size ripple within the range of 1200 Hz.

To evaluate the impact of low-frequency ripple, Figure 2 presents a frequency scan using a finer step size of 60 Hz in the range up to approximately 1200 Hz. The ripple amplitude is set to 5% of the electron beam's RMS size in both transverse planes.

The simulation results show that vertical emittance growth is accompanied by a corresponding decrease in horizontal emittance. The severe emittance transfer occurs at low frequencies, while its impact diminishes rapidly at higher frequencies.

ALLOWABLE TOLERANCE AT 60 Hz

The strong response observed around 60 Hz is particularly concerning, as the standard AC power line frequency in the US is 60 Hz.

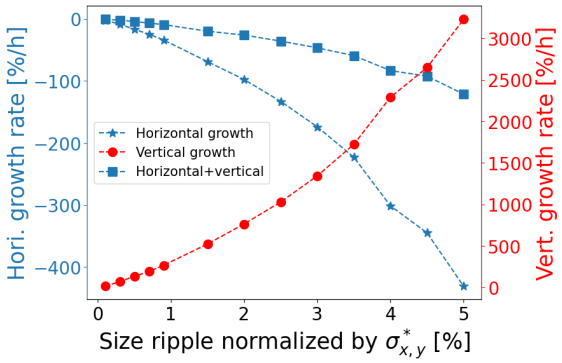

Figure 3: Proton emittance growth rates for different magnitudes of electron size ripple. The horizontal and vertical emittance growth rates are shown separately, along with the combined growth rate for the summation of horizontal and vertical emittance (H+V).

Figure 3 illustrates the horizontal and vertical emittance growth rates as a function of the electron size ripple magnitude. The center frequency and the bandwidth are set to 60 Hz. The figure also presents the combined growth rate, defined as the summation of horizontal and vertical emittance growth (H+V). While the horizontal and vertical emittance growth rates show significant variation with increasing ripple magnitude, the combined growth rate remains much more stable across all cases. This stability indicates that there is emittance transfer between the horizontal and vertical planes. The conservation of the total emittance (H+V) highlights its role as a better conserved quantity in the presence of electron size ripple.

Assuming an emittance growth threshold of 10%/h, the allowable electron size ripple is estimated to be in the range of 0.1% – 0.2%. This sets a stringent requirement on quadrupole power supply [5].

MECHANISM OF EMITTANCE TRANSFER

Unequal transverse emittances and electron size ripple are essential ingredients for driving emittance transfer. The emittance transfer induced by electron size ripple also depends on the transverse working point. Figure 4 shows the proton emittance growth rates across various transverse working points under a 0.5% electron size ripple. A clear diagonal pattern emerges in the tune space: working points along the same diagonal line exhibit similar emittance growth rates. This pattern directly indicates that emittance growth and transfer are driven by synchro-betatron resonances, specifically those of the form $2\nu_x - 2\nu_y + p\nu_z = 0$. The results also reveal that vertical emittance growth rates are more sensitive to the transverse working point, highlighting the possibility of optimizing the working point to suppress vertical emittance growth.

Figure 5 illustrates the proton emittance growth rates as a function of proton bunch length and momentum spread in the presence of a 5% electron size ripple. Reducing either the

ISBN: 978-3-95450-261-5 ISSN: 2673-7000 doi: 10.18429/JACoW-NAPAC2025-TUP050

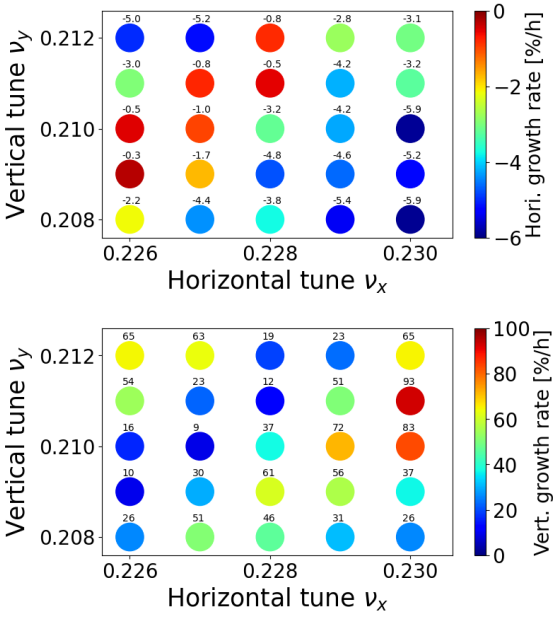

Figure 4: Proton emittance growth rates at different working points with a 0.5% electron size ripple. The fitted growth rates, in units of %/h, are labeled on the plot.

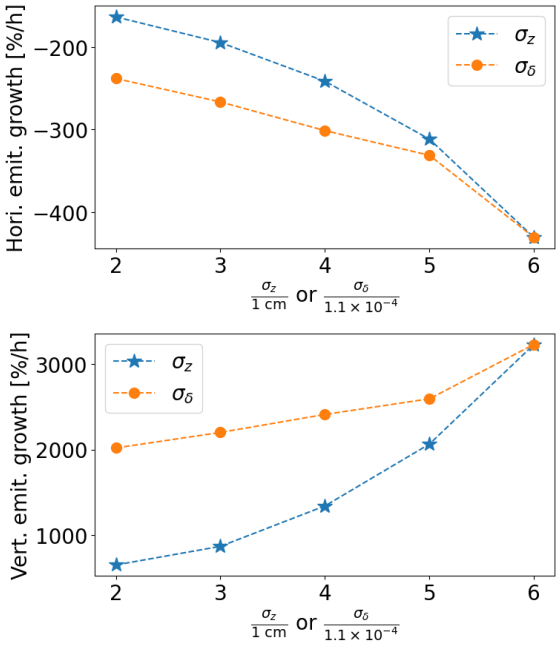

Figure 5: Proton emittance growth rates for different proton bunch lengths and momentum spreads under a 5% electron size ripple. The impact of reducing the bunch length and momentum spread on mitigating emittance transfer is illustrated.

bunch length or the momentum spread decreases emittance transfer between the horizontal and vertical planes. Among the two strategies, shortening the bunch length proves to be more effective. This is because shorter bunch lengths not only reduce the longitudinal action but also mitigate the hour-glass effect.

Compared to electron orbit ripple, electron size ripple of the same amplitude induces significantly larger emittance transfer. This distinction arises because electron size ripple not only causes proton diffusion through beam-beam interactions but also modulates the proton betatron tunes.

To understand why ripple near 60 Hz is particularly harmful, and to explore how tune modulation enhances emittance growth, we introduce a simplified model to study beam dynamics near a synchro-betatron resonance.

The effective Hamiltonian governing the coupled motion near the synchro-betatron resonance is given by:

$$h = \mu_x J_x + \mu_y J_y + \mu_z J_z + \frac{\lambda \mu_t}{\sin \mu_t} J_x J_y J_z^2 \sin\left(2\phi_x - 2\phi_y + 4\phi_z + \mu_t\right)$$

where $\mu_t = \mu_x - \mu_y + 2\mu_z$ denotes the detuning from the resonance condition.

The vertical action J_y is resolved by a symplectic ODE solver [6]. Figure 6 shows the fitted growth of J_y when μ_t is modulated. A fractal-like structure emerges when scanning the modulation frequency and amplitude.

Notably, the frequency 60 Hz lies within the center of the chaotic layer. This may explain why the strongest emittance growth in the presence of electron size ripple occurs at low frequencies, particularly around the AC line frequency. For higher power-line harmonics, starting with 360 Hz, the effect

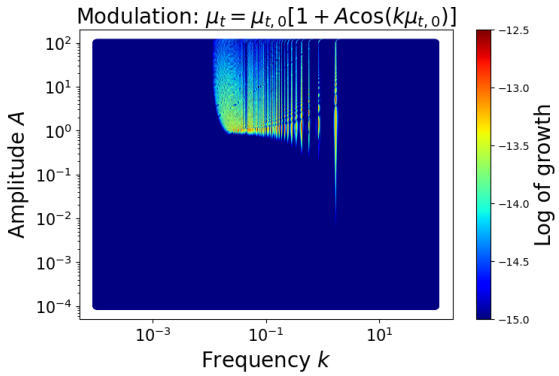

Figure 6: Growth of vertical action under tune modulation near the synchro-betatron resonance. The nominal working point is used, and $\mu_{t,0} = 2\pi\left(\nu_x - \nu_y + 2\nu_z\right) = -0.004\pi$, corresponding to 156 Hz. The initial action is chosen as $J_x = \epsilon_x, J_y = \epsilon_y$.

of the size ripple is predicted to be much lower, even before the eddy current effects are taken into account.

CONCLUSION

Electron size ripple induces strong emittance transfer in the EIC. Simulations and modeling show that ripple above 0.2% causes unacceptable growth. Mitigation requires tight ripple control, careful optimization of working point, and further development of a dynamic focusing scheme to suppress the synchro-betatron resonance [7].

ISBN: 978-3-95450-261-5 ISSN: 2673-7000 doi: 10.18429/JACoW-NAPAC2025-TUP050

REFERENCES

[1] F. Willeke and J. Beebe-Wang, "Electron ion collider conceptual design report 2021", Brookhaven National Lab., Upton, NY, USA; Thomas Jefferson National Accelerator Facility, Newport News, VA, USA, Tech. Rep. BNL-221006-2021-FORE, 2021. doi:10.2172/1765663

[2] Y. Luo, D. Xu, M. Blaskiewicz, and C. Montag, "Experimental demonstration of a large transverse emittance ratio 11 : 1 in the Relativistic Heavy Ion Collider for the Electron-Ion Collider", *Phys. Rev. Lett.*, vol. 132, no. 20, p. 205 001, 2024. doi:10.1103/PhysRevLett.132.205001

[3] D. Xu *et al.*, "Effect of electron orbit ripple on proton emittance growth in EIC", in *Proc. IPAC'23*, Venice, Italy, May 2023, pp. 108–111. doi:10.18429/JACoW-IPAC2023-MOPA039

[4] B. Podobedov and M. Blaskiewicz, "Eddy current shielding of the magnetic field ripple in the EIC electron storage ring vacuum chambers", Brookhaven National Lab., Upton, NY, USA, Tech. Rep. BNL-224904-2023-TECH, 2023. doi:10.2172/2203273

[5] B. Podobedov *et al.*, "Physics-driven specifications for the EIC ESR magnet power supply ripple", in *Proc. IPAC'25*, Taipei, Taiwan, Jun. 2025, paper MOPS065, to be published.

[6] C. Rackauckas and Q. Nie, "DifferentialEquations.jl–a performant and feature-rich ecosystem for solving differential equations in Julia", *J. Open Res. Software*, vol. 5, no. 1, p. 15, 2017. doi:10.5334/jors.151

[7] D. Xu *et al.*, "Dynamic focusing to suppress emittance transfer in crab-crossing flat beam collisions", Jun. 2025, arXiv:2506.21289 [physics.acc-ph]. doi:10.48550/arXiv.2506.21289